Proceedings World Geothermal Congress 2020+1
Reykjavik, Iceland, April - October 2021

Design, Simulation, and Construction of a Modular Desalination Plant with Low Enthalpy Geothermal Energy in Baja California Sur, Mexico

Héctor AVIÑA[1], Luis Antonio GONZÁLEZ[1, 2], Inti RAMOS[1 *], Selef GARCIA[1]

[1]Grupo iiDEA, Instituto de Ingeniería, Universidad Nacional Autónoma de México, Circuito Escolar, Ciudad Universitaria, C.P. 04510, CDMX. Tel: (55) 56233500 Ext. 1656.
*Correo: ORamosC@iingen.unam.mx

[2]Facultad de Ingeniería, Universidad Autónoma de Baja California, Blvd. Benito Juárez S/N, CP 21280, B.C. Tel: (686) 566-4270.

Keywords: MED, direct use, low enthalpy geothermal, freshwater, desalination

ABSTRACT

This paper shows the results of the design, simulation, and construction of a Geothermal Modular Desalination Plant (DMG). Through the collaboration of the Autonomous University of Baja California (UABC) and the IIDEA applied research group of the National Autonomous University of Mexico (UNAM), they have worked with the objective of solving social problems such as the shortage of drinking water in the Mexican territory. One of the great challenges that this association has faced is the shortage of drinking water in the peninsula of Baja California Sur. Laboratory tests of the system were carried out, and exploration work was carried out by the IIDEA group in two geothermal wells in the Diamond Development Complex, in Los Cabos BCS. There is a volumetric flow register of 16 liters per second and whose temperature is 90 °C. With this resource, it is possible to activate the DMG and obtain a volume of drinking water of 40 cubic meters per day. This volume is sufficient for more than 265 families, according to the WHO figures of 150 liters/person/day and widens the opportunities for Development of low enthalpy geothermal energy in Mexico. This contributes to the dissemination of direct uses, human resources training, and providing innovative solutions to the basic needs of the population.

1. INTRODUCTION

Water is a vital resource for life on the planet we inhabit, although the Earth's surface is made up of 2/3 of water, only 0.77% is freshwater accessible for human consumption. This percentage is distributed in the continents, but not equitably. This factor, as well as population growth, climate change, inadequate water management, and lack of quality infrastructure for distribution, has influenced the accelerated increase in regions with a shortage of Water.

Global water use has multiplied by six in the last 100 years and continues to grow steadily at an approximate annual rate of 1% (Wada, 2016; AQUASTAT, s.f .; cited by WWAP, 2018). Figure 1 shows the regions of the world with water scarcity, where you can see the situation of the peninsula of Baja California, which in general is in a state of severe water shortage. Also, the trend for 2050 is not favorable, as a continuous increase in the scarcity of the precious water resource is projected.

Drought and scarcity may seem the same, but they are concepts that represent different phenomena. Drought is a natural phenomenon that ends (in all its manifestations) when the rains arrive, and the normal level of the bodies of water is recovered. On the other hand, the shortage can persist with or without rains and without drought occurring. This phenomenon is due to human action and consists of extracting and consuming more water than can be recharged from the one in existence and its disposition (Esparza, 2014).

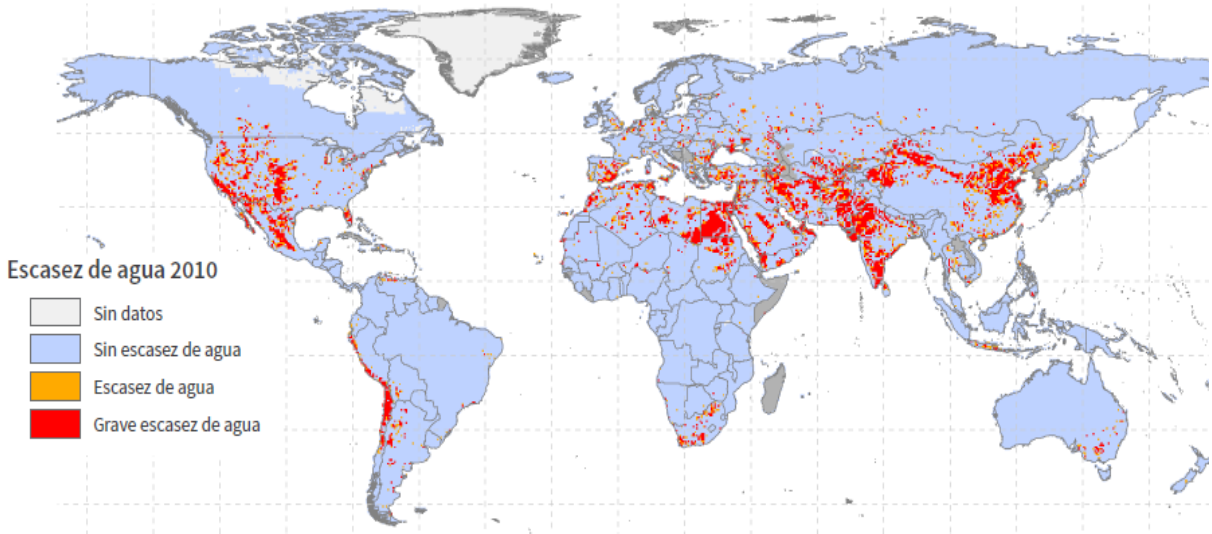

Figure 1: Physical map of water scarcity in2010 (WWAP, 2018).

Desalination is an increasingly used technology, especially since various circumstances combine. Firstly, the demand for water will increase exponentially, while freshwater reserves will begin to collapse. Second, desalination prices continue to decrease, and the technological effectiveness of desalination methods and processes continues to increase.

The desalination system consists of feeding brackish or marine water to a desalination plant. Its function is to condition and eliminate salts in the water to obtain a product and rejection or brine.

There are several technologies currently developed to desalinate seawater. Although they have different characteristics according to the type of energy, design, and production that each requires, all have the same objective, reduce the concentration of dissolved salts of seawater. This allows distinguishing between the processes that separate the water from the salts and those that actually affect the separation of the salts from the solution (Dévora, González & Ponce, 2012). Table 1 shows the types of desalination.

Table 1: Desalination technologies.

Separation	*Energy*	*Process*	*Method*
Saltwater	Thermal	Evaporation	Sudden Distillation (Flash)
			Multi-effect distillation
			Thermo vapor compression
			Solar distillation
		Crystallization	Freezing
			Hydrate formation
		Filtration and evaporation	Membrane distillation
Water salts	Mechanic	Evaporation	Mechanical vapor compression
		Filtration	Inverse osmosis
	Electric	Selective filtration	Electrodialysis
		Chemistry	Ion exchange

The use of desalination plants in Baja California is not something new; such technologies have been developed in recent decades. The first desalination plant was located in Baja California, considered one of the largest worldwide with a capacity of 320 liters per second (lps), 27,648 m3 / day (Arreguín & López, 2015).

Desalination costs vary depending on factors such as the desalination process, source water quality, water quality demanded by users, plant capacity, plant operation and maintenance, installation site conditions, and energy costs, to mention the most relevant ones. Considering that energy is one of the factors that influence the costs of desalination, the implementation of alternative energy provides the opportunity to reduce costs in this area. It is important to highlight the use of renewable energy sources to boost desalination processes depending on the conditions and operating parameters that affect water production levels. These include solar, geothermal, wind, and oceanic (Alkaisi, Mossad & Sharifian-Barforoush, 2017; Abdelkareem, El Haj Assad, Sayed & Soudan, 2018; Ghaffour, Bundschuh, Mahmoudi & Goosen 2015). Despite the existing potential, renewable energy-driven desalination systems are rare. They only represent about 0.02% of the total desalination capacity. Nevertheless, an increase in this percentage is projected, due to the significant reduction in the costs of renewable energy systems, as well as the increase in fossil fuel prices (Ghaffour et al., 2015). Another advantage of using renewable energies is that they are normally easier to operate and maintain. In addition, the power plants are generally located in coastal areas where renewable energy sources are available (Ismail, Azab, Elkady & Abo, 2016).

Due to the benefits of renewable energy and the geothermal manifestations present in the town of Puertecitos, it's been decided to select said energy as a trigger source of the distillation system due to multiple effects of low enthalpy. The main advantage of geothermal energy is primarily that thermal storage is unnecessary in such systems. Second, the energy production of these resources is generally invariant with fewer intermittency problems (compared to solar and wind energy). High exploration costs, high investment risk, and high installation costs are disadvantages if new geothermal reservoirs are targeted. However, low enthalpy geothermal heat is much less expensive due to less drilling required (Bourouni & Chaibi, 2005; Ghaffour et al., 2015). Several configurations can be used to couple of geothermal energy with desalination processes (Ghaffour et al., 2014).

In the world, desalination by thermal methods has had a strong development in Arabic countries where oil is abundant, but water is scarce (Nava & Hiriart Le Bert, 2008). Around 70% of all desalination in the GCC (Gulf Cooperation Council) is based on thermal processes (B2B Connect UAE, 2018).

The region of Baja California is geologically complex since it houses the tectonic border between the North American and Pacific plates (Vázquez-Figueroa et al., 2009). This encourages the area to have geothermal activity (Suárez, 2004; Hiriart Le Bert, 2009). Báncora and Prol (2006) made a map showing the anomalies of heat flow in the Peninsula of Baja California and the Gulf of California, they said the map was prepared using direct measurements and estimated values.

The Geothermal potential of Baja California has been well known for examples such as the developments of Cerro Prieto and Las Tres Vírgenes. However, conventional exploration studies have focused on the Los Cabos area, which may seem to comprise an important geothermal resource. Recent research on the coast of hydrothermal systems on the Baja California peninsula provides evidence of the anomalies in the Los Cabos area, Baja California Sur (López-Sánchez et al., 2006).

Los Cabos is an important touristic center; however, the peninsula of California is relatively disconnected from the rest of Mexico and the hydrocarbon supplement in this region is relatively expensive. Tourism development has caused a growth in population and demand for water. Hot water was found during the well drilling process to supplement a desalination plant in Los Cabos San Lucas, probably related to hydrothermal systems. In this way, geothermal energy has been considered as a solution to the problems of energy and water supply, as one the possibility of using geothermal energy for some of the electrical needs and in desalination processes (López-Sánchez et al., 2006).

López-Sánchez et al. (2006) were the first ones to report geothermal activity in the Los Cabos area (Cabo San Lucas and San José de Los Cabos), the southernmost part of the peninsula (Figure 1). Three wells were drilled in the Los Cabos area, and these authors analyzed five geochemical samples of these. From these samples, two turned out to be geothermal waters (LC-4 and LC-5, Figure 2) and two others were cold water (LC-1 and LC-2), only a few meters apart between them.

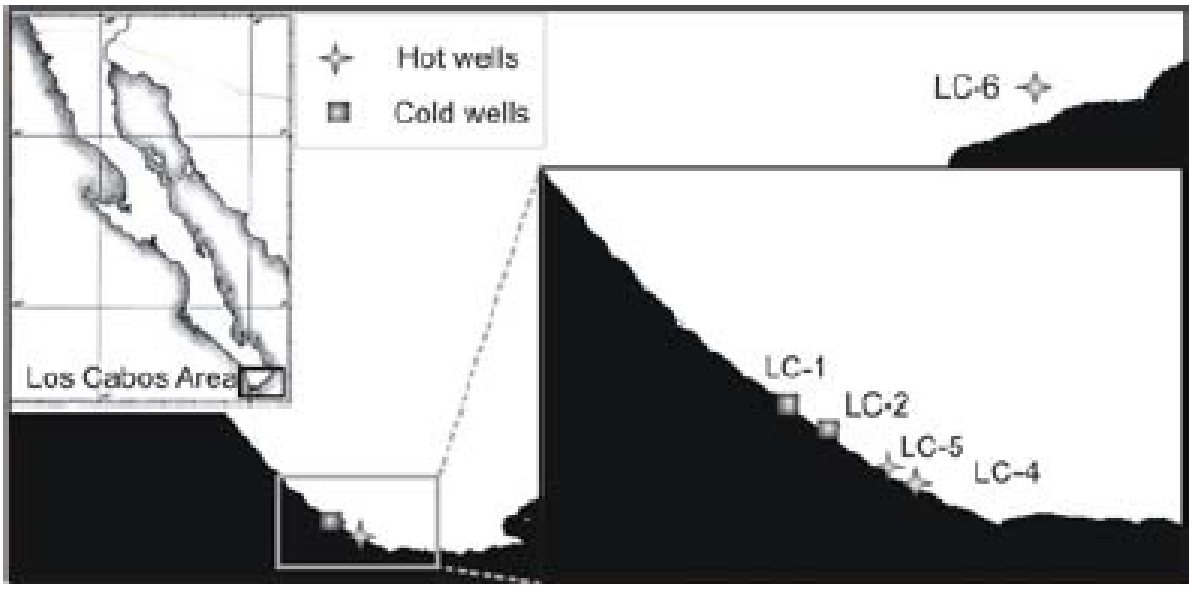

Figure 2: Location of the Los Cabos area and the hot water wells on the coast. Taken from López-Sánchez et al. (2006).

2. DESCRIPTION OF THE GEOTHERMAL RESOURCE

Schaaf et al. (2000) suggest a magmatic relationship between the Los Cabos block and the Puerto Vallarta Batolito in Jalisco, associating the La Paz fault with an accretional structure of the Los Cabos Block with the Baja California peninsula. This way, the Batolito of Puerto Vallarta and the Los Cabos Block separated from each other in a movement that originated the Gulf of California during the Miocene (Figure 2). Because of this movement, the Baja California Peninsula was separated from the North American plate and accreted to the Pacific plate during the Miocene (López-Sánchez et al., 2006). Also, the Pacific plate has been transported 640-720 km northwest from 12.3 Ma (Atwater and Stock, 1998).

The regional tectonics in Baja California are strongly related to the geodynamic development of the Gulf of California and the extension with a lateral component. This lateral component is recognized by several researchers in two different kinematic phases of shear at the plate boundary (Figure 3). During the first phase, it is well known that the gulf began its opening by an orthogonal rifting and mainly with a dextral shear that was partitioned into faults west of the Baja (Figure 2A). It is known that the current transtensional strain regime was established in the Gulf of California at 6 Ma (Figure 2B and C, Fletcher et al., 2007).

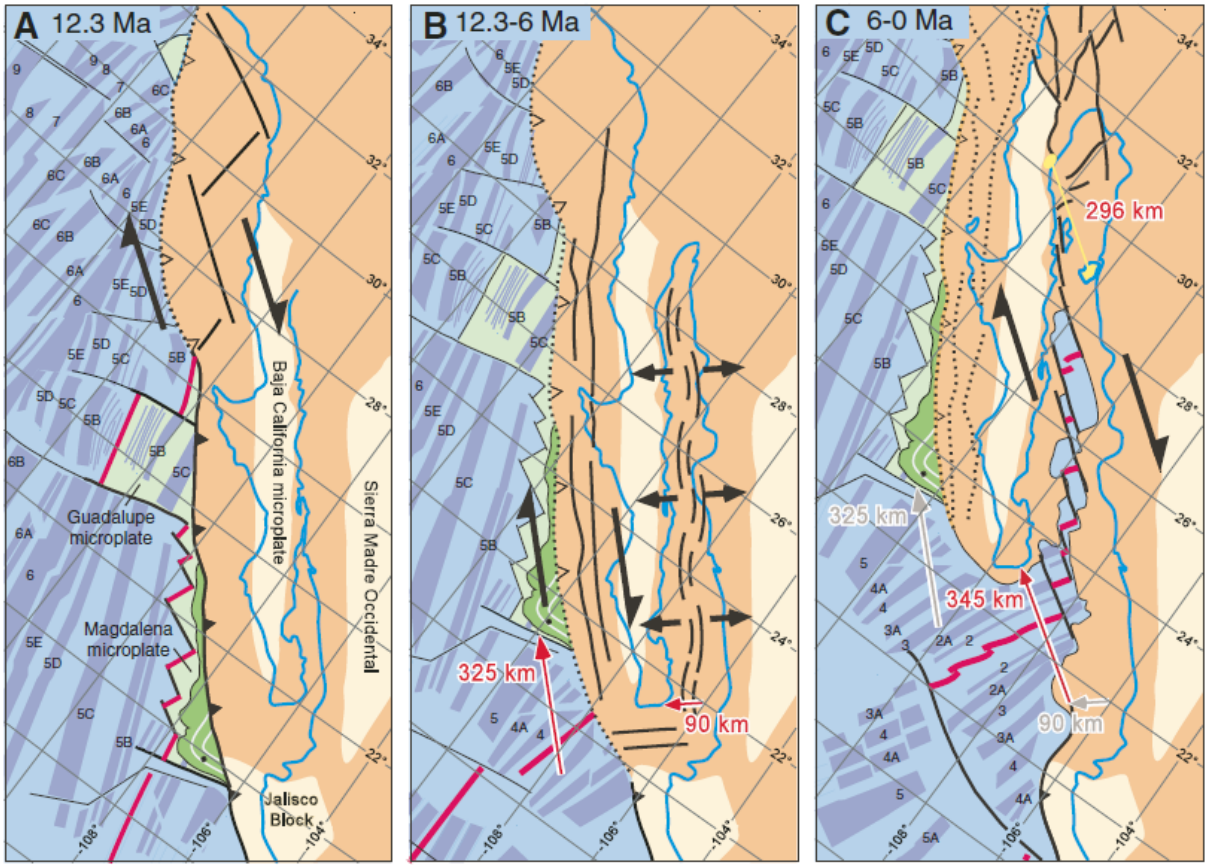

Figure 3: Tectonic map of the two-phase kinematic evolution model of the shear margin of the North American and Pacific plates. A) Active configuration of the western crest segment of Baja California just before being abandoned at 12.3 Ma. B) The plate movement between 12.3 and 6 Ma was kinematically partitioned in a lateral dextral displacement (325 km) in faults at the west of Baja California and on an orthogonal rifting in the Gulf of California (90 km). This is known as the protogulf rifting phase. C) From 6 to 0 Ma the failure to the west of Baja California ceased, and all the movement of the plate was located in the Gulf of California, which accommodated 345 km of a transtensional shear. Taken from Fletcher et al. (2007).

The result of this geodynamic context is the formation of a young ocean basin. It was dissected by transforming faults east of Baja California, while to the west of Baja California Sur is the Magdalena continental shelf. To the southwest of the Magdalena platform is the Todos Santos submarine basin (Figure 4), where the area of geothermal interest is located. The Todos Santos basin contains numerous underwater canyons and fault escarpments (Figure 3, Fletcher et al., 2007).

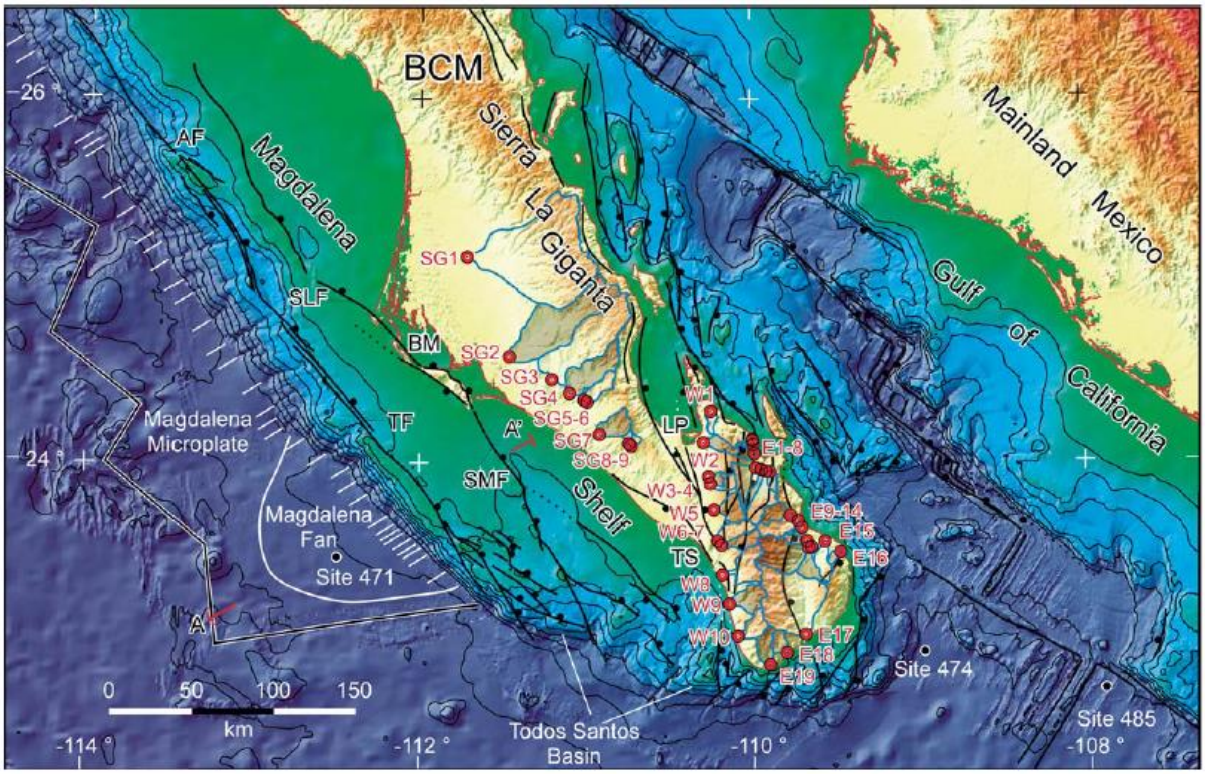

Figure 4. Map of the relief configuration in southern Baja California. It is located between two main shear zones on the margin of plates in the Gulf of California and the Magdalena platform. The structural configuration of marine and continental faults. Taken from Fletcher et al. (2007).

With this tectonic framework, a high geothermal gradient is expected as a result of the thermal anomaly of the mantle in the area, verified by the hot wells reported in the Los Cabos area (Figure 5). In addition to the hydrothermal manifestations coincide with the transtensional failure system (López-Sánchez et al., 2006).

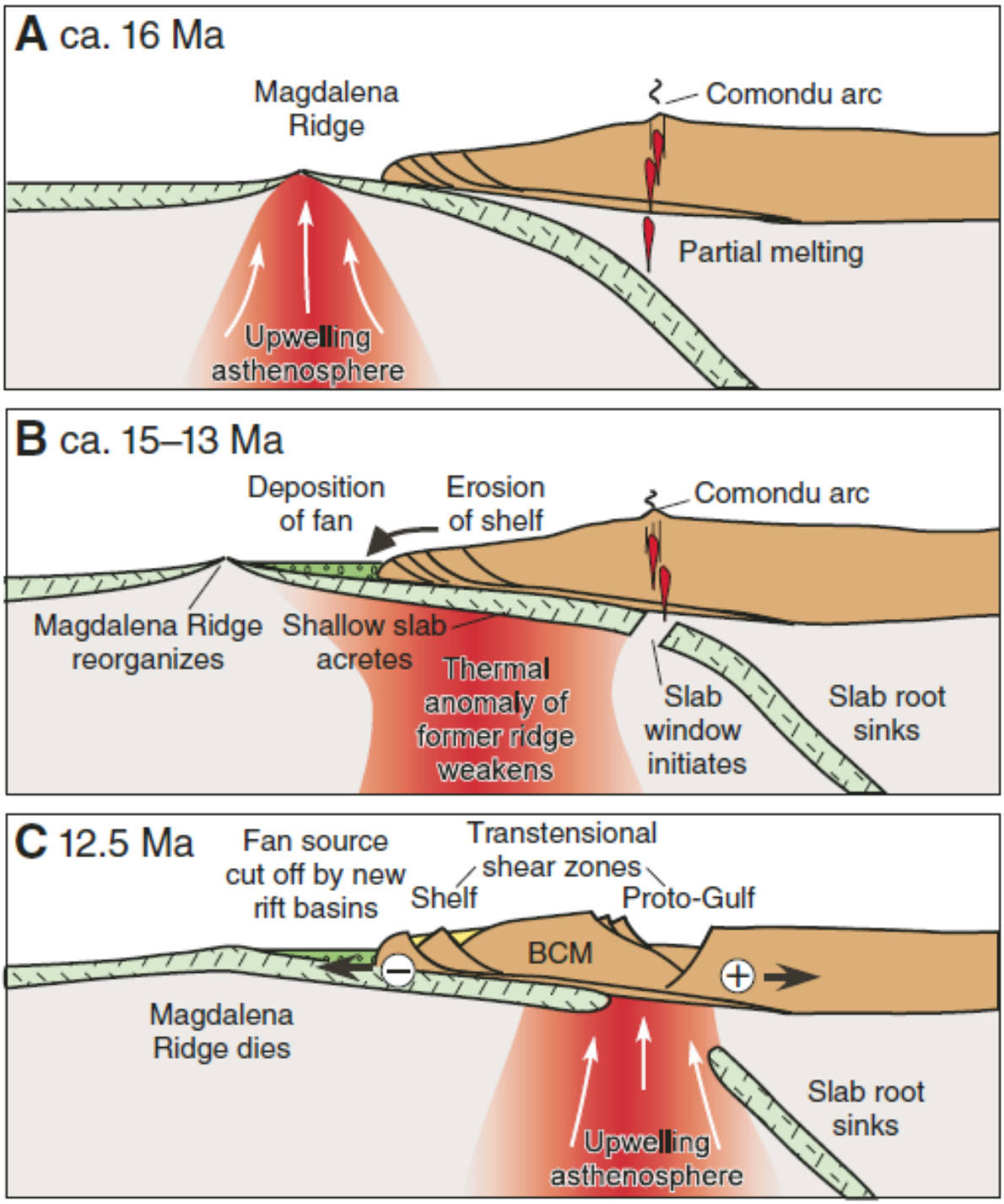

Figure 5: Schematic section of the western paleotrinchera of Baja California Sur, showing the tectonic evolution of the Magdalena platform. A) The Magdalena dorsal converges in the trench of Baja California at 16 Ma. B) The horizontal subduction under the North American plate is fragmented, while the Magdalena platform continued to rise and erode due to the increase of the mantle bulge. C) The expansion rate of the Magdalena dorsal decreased, and the subduction window caused a rise in the mantle, focused on the margin of deformation of the protogolfo of California. Taken from Fletcher et al. (2007).

2.1 Process description.

Multi-effect distillation, represented in Figure 6, is the oldest procedure. It is normally used to desalinate large volumes of seawater. The principle of this process is based on the fact that the amount of energy that can be stored in the water at its boiling temperature decreases when the pressure decreases. That is why when sea or brackish water at its boiling temperature flows to a container with lower pressure, the excess energy contained in the liquid causes evaporation. This flow of energy that comes out of the liquid causes the temperature of the sea or brackish water to drop to the corresponding value to that of saturation at that new pressure (Arreguín & Martín, 2000). When evaluating the problem of water resource scarcity in small ports and the low availability of electricity, it is considered as a solution the implementation of the multi-effect distillation technology of low enthalpy activated with geothermal energy for desalination. For this reason, the simulation of the proposed system for the community of approximately 80 people is presented.

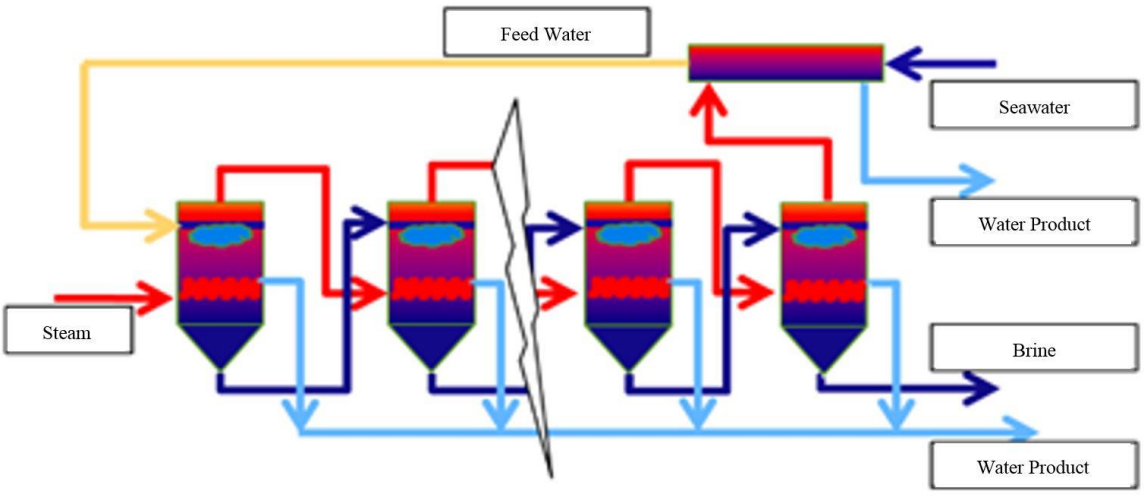

Figure 6: Multiple Effect Evaporation Plant.

2.2 MED-LE System Modeling and Simulation

The thermodynamic model of the MED-LE is based on the hypothesis and analysis proposed by Geankoplis (2003) and the modifications made by Ettouney (2007).

In order to calculate the temperature drop through each of the effects, the following relationship is obtained:

$$\Delta T_t = T_S - (n-1)\Delta T_\ell - T_{bn}$$

The temperature drop in the first effect is obtained by:

$$\mathrm{T_1} = \frac{\Delta \mathrm{T_1}}{\mathrm{U_1} \sum_{\mathrm{i=1}}^{\mathrm{n}} \frac{1}{\mathrm{U_i}}}$$

In the same way, the temperature decrease in the 2-n effects is obtained:

$$\Delta T_i = \Delta T_1 U_1 / U_1$$

The brine temperature in the first effect is obtained from the ratio:

$$T_{b1} = T_s - \Delta T_1$$

To calculate the brine temperature of the effects from 2 to n:

$$T_{bi} = T_{bi-1} - \frac{\Delta T_1 U_1}{U_1} - \Delta T_\ell$$

Distillate flow in the first effect:

$$D_1 = M_d / \left(\lambda_{v1} \left(\frac{1}{\lambda_{v1}} \frac{1}{\lambda_{v2}} + \cdots \ldots \ldots \cdots \frac{1}{\lambda_{vn-1}} \frac{1}{\lambda_{vn}} \right) \right)$$

Distillate flow in the effects of 2 to n:

$$D_i = D_1 \frac{\lambda_{v1}}{\lambda_{vi}}$$

Brine flow of effect 1 to n:

$$B_i = X_{cw} D_i / (X_{ci} - X_{cw})$$

Feed flow in the effects of 1 to n:

$$F_i = D_i + B_i$$

Heat transfer area in the first effect:

$$A_1 = \left(\frac{D_1 \lambda_{v1}}{U_1 (T_s - T_{b1})} \right)$$

Heat transfer area in the effects of 2 to n:

$$A_i = \frac{D_i \lambda_i}{U_i (T_{vi-1} - T_{bi})}$$

Amount of steam flow:

$$M_s = D_1 \frac{\lambda_{v1}}{\lambda_s}$$

Condenser heat transfer area:

$$A_c = \frac{D_n \lambda_n}{U_c (LMTD)_C}$$

Calculation of seawater flow for cooling:

$$D_n \lambda_{vn} = (M_f + M_{cw}) C_p (T_f - T_{cw})$$

The MED-LE system model is considered under the following assumptions (Khalid, Antar, Khalifa & Hamed, 2018):

• The steam is pure (without salt) since mist eliminators do not allow the brine to be carried away with the steam formed.

• The effects do not lose energy in the environment, which is a common assumption in the literature.

• The same thermal load in all effects except the first one.

• Constant values of boiling point elevation, thermal losses associated with the pressure drop (flow inside the tubes and the defogger as well as losses associated with condensation in addition to the non-equilibrium range) due to the small temperature range.

• Constant specific heat due to low-temperature range.

• The feed that enters the first effect has 5 ° subcooling (below its saturation temperature).

• Evaporator tubes are completely wetted by sprayed seawater, and there are no dry patches.

The simulation of the desalination system activated with low enthalpy geothermal energy was carried out with ASPEN®, which is a set of process modeling programs. One of these programs is ASPEN Plus, which allows the modeling of steady-state processes. The user interface is based on a library of component models, based on Fortran. This library is editable by the user by connecting these components with the material, heat, working currents, and providing input values. It allowed modeling the multi-effect distillation system to be developed. It considered the variables presented in Table 2 to perform the validation of the simulator through the work carried out by Manenti et al. (2013), obtaining the results presented in Table 2.

Table 2: Simulation Variables.

Parameter	Valor
Seawater temperature	25°C
Geothermal resource temperature	124°C
Last effect temperature	40°C
Heat transfer area per camera	1,000 m^2
Salinity of seawater	35,000 ppm
Brine	70,000 ppm
Thermodynamic losses	2°C
Total distillate flow	12 kg/s

Table 3: Validation Results.

Parameter	Manenti et al.			Simulation performed González-Uribe et al.		
	1er Effect	2do Effect	3er Effect	1er Effect	2do Effect	3er Effect
Energy (MJ / s)	15.785	6.6724	7.5861	15.7516	6.2745	7.3996
Hot fluid temperature (° C)	112.271	105.281	88.255	109.982	105.164	82.151
Cold fluid temperature (° C)	112.839	102.297	86.571	109.681	98.548	81.653
Liquid fraction of the hot fluid	1.00	0.507	1.00	1.00	0.498	1.00
The liquid fraction of the cold fluid	0.7513	0.812	0.740	0.7605	0.8210	0.7503
Exchanger value U * A (kW / K)	1040	1040	1040	1382.27	850	605.082
Effectiveness of the heat exchanger area (m2)	1000	1000	1000	1382.27	850	605.082
Factor (LMTD correction)	0.191	0.975	0.931	0.191	0.975	0.931
LMTD of the heat exchanger (° C)	15.178	6.415	7.294	15.178	6.415	7.294
Convergence tolerance	0.0001	0.0001	0.0001	0.0001	0.0001	0.0001

When analyzing the results of the validation carried out under the same tolerance conditions in the convergence of the data, an average difference of 2.87% was determined with respect to the calculation of the amount of energy required to generate the two-phase fLuid in the water circuit at sea. According to the temperature values of the hot and cold fluid, an average difference of less than 3.02% and 4.04% respectively was found for each of the effects. In the liquid fraction of the hot and cold fluid a difference was observed for below 1.91% and 1.33% respectively compared to the results presented by Manenti et al. (2013).

3. RESULTS AND DISCUSSIONS

Once the simulator was validated and obtained satisfactory results, the simulation was carried out, see Figure 7, according to the needs of the small village where the supply of water resources for 80 people will be considered. Taking as a reference consumption of 150 liters/day/room the simulation was carried out looking for a capacity of 12,000 liters/day. Once the population's needs were determined, the initial conditions of the data collected from the studies at the site average seawater temperature at the entrance 32 ° C were introduced to the simulator.

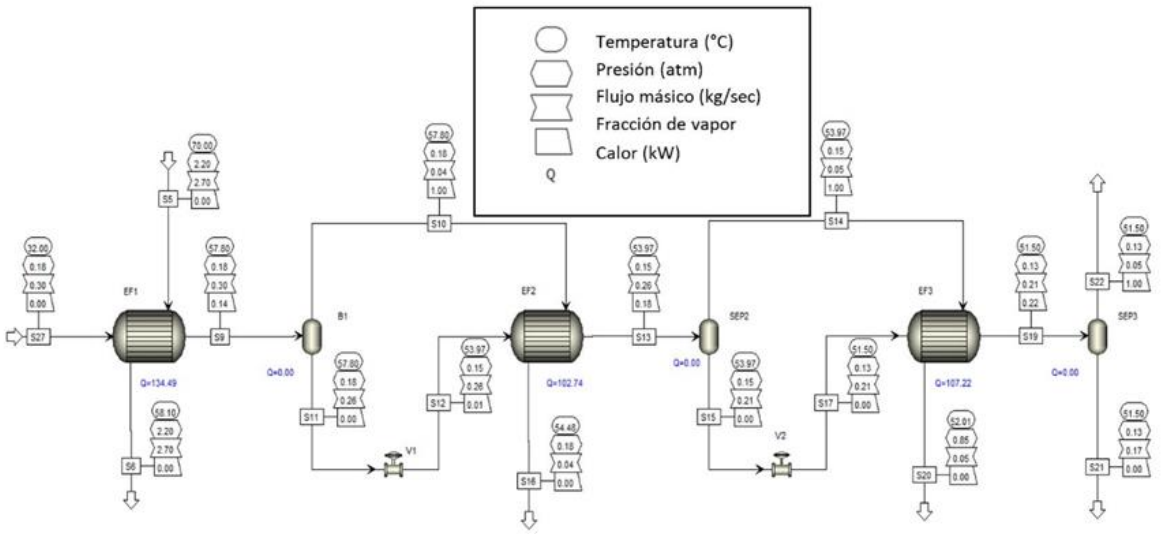

Figure 7: Simulation of the MED-LE system for small doors.

The temperature of the geothermal resource available in the region is in the range of 70 to 228 ° C, the salinity of seawater at the inlet is 34,500 ppm.

After collecting the data, it was proceeded to the parametric analysis of the most important variables for the MED-LE system. Thus, it would be able to examine in detail its behavior and the impact of each of the effects for the generation of distilled water.

When changing the temperature of the geothermal resource, it is necessary at least 60 ° C to activate the distillation system. It was also found by simulation that the appropriate operating temperature should be in the order of 70 ° C, with a Desalination water production capacity of 0.1393 kg / s. If the temperature rises to the level of 74.78 ° C the exponential is cut, since the distillation process is inhibited due to the pressure levels in each of the chambers.

This produces a dangerous approach of crystallization in the brine since the cycle is carried out in series from chamber 1 to the subsequent one. So, it was determined as the maximum operating temperature of the system to be 75 ° C, as shown in Figure 8.

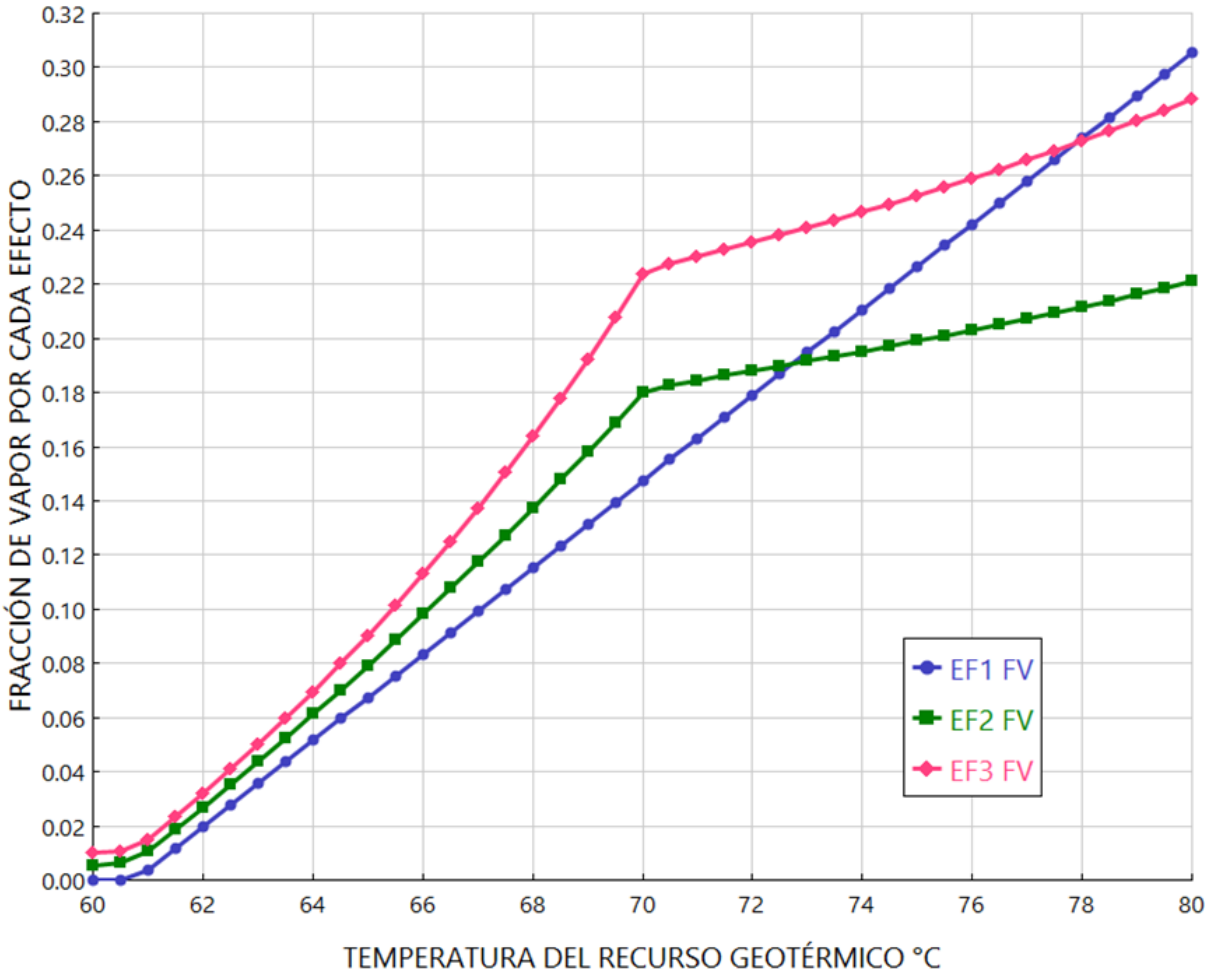

Figure 8: Vapor fraction by an effect.

Once the nominal operating temperature of the system was defined, the variation of seawater temperature was carried out finding a system production capacity of 0.126-0.1393 kg / s, as shown in Figure 9.

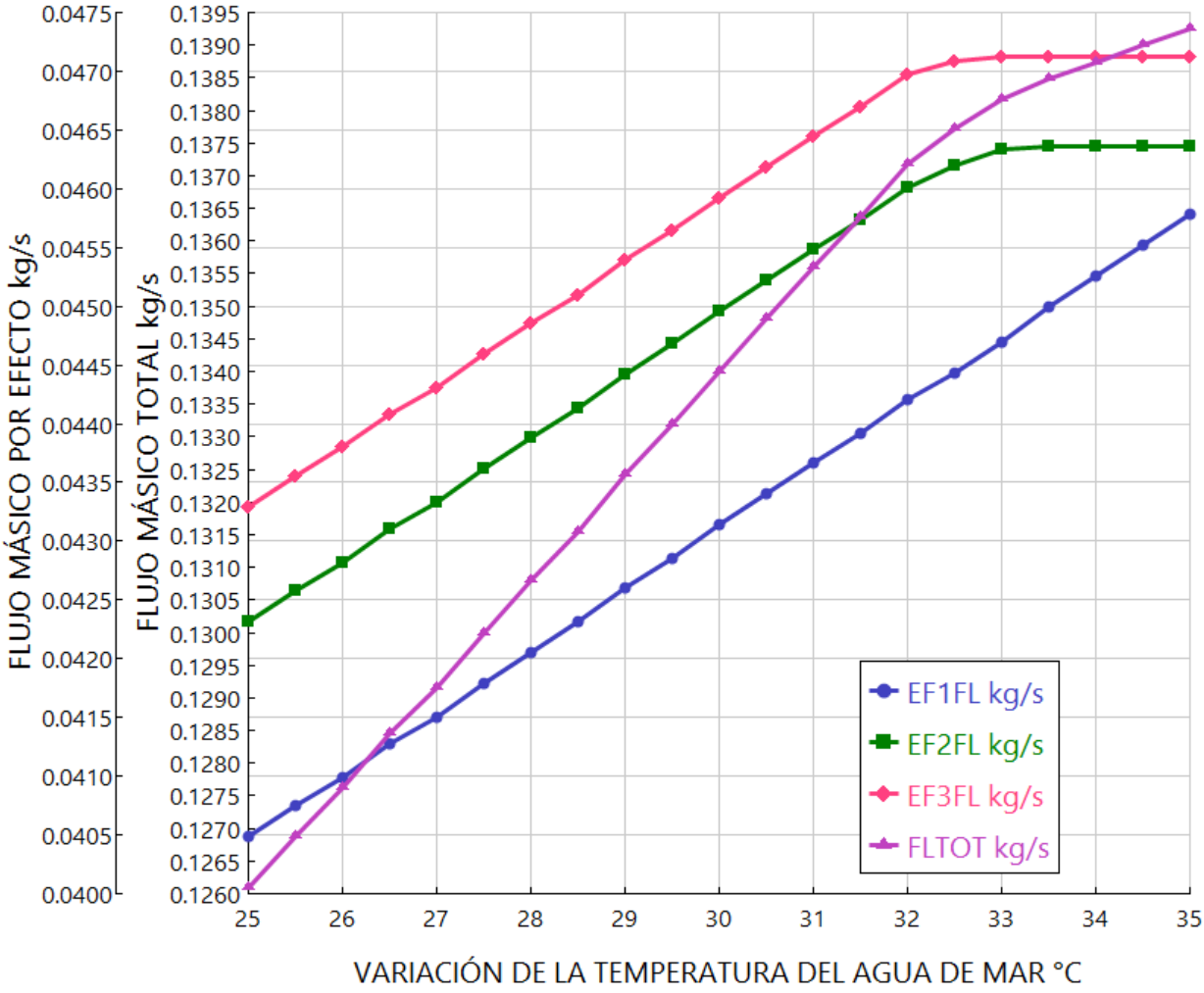

Figure 9: Mass water flow product.

Once the equipment identified the possible water production margin, a variation was also made with the mass flow of seawater of 0-0.40 kg / s. This can be seen in Figure 10, identifying that a water flow of 0.18 kg / s is required to produce the maximum amount of distillate with the amount of energy available for the equipment, this with a minimum area of heat transfer per chamber 50 m^2.

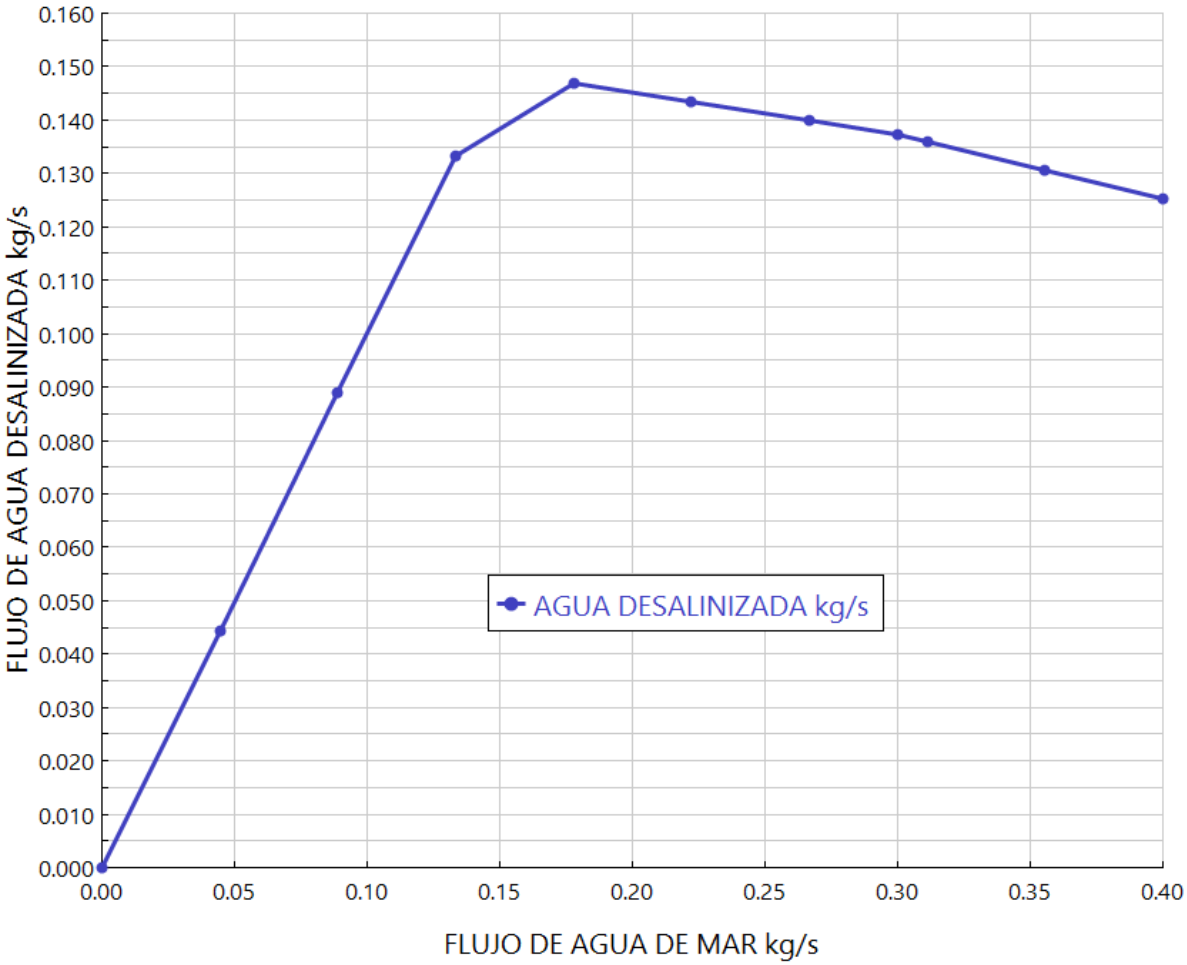

Figure 10: Desalinated water production.

4. CONCLUSION

The effective use of geothermal resources presented in this document includes the direct use of geothermal energy for the activation of a desalination unit. The innovative approach of our research is the coupling of two mature and well-proven technologies (geothermal and multi-effect distillation). The key findings of the energy analysis showed that purified water could be produced at a comparable level with respect to the cost as a freshwater of current water resources (groundwater and surface water). By means of the mathematical analysis, it is possible to predict the energy required for the injection of the concentrate obtained from the desalination process in the tank with geothermal water flow. It has also been shown that as the amount of concentrate injected increases when there is positive pressure in the reservoir, the flow resistance in the injection well increases. This increase can lead to a constant increase in the required injection pressure during long-term operation. As a result, the demand for energy also increases. The key aspects are the need to maintain as much as possible the segregation of the physical phenomena involved in the start-up phase in order to avoid all the possibilities of redundant effects that can lead to process instabilities and, therefore, to an uncontrollable process. Special attention is paid to the need to preserve the wet conditions of the tube bundle within the effects, especially with geothermal sources that are not directly manageable. Also to the progressive stabilization of the effects along the distillation train, since dynamics can induce strong variations to downstream units. The integration presented also causes economic savings in the cost of freshwater produced with respect to conventional technology.

Acknowledgment

The authors extend their thankfulness to CONACYT for their support through the P11 project "Technological development for the use of low enthalpy geothermal energy" of the CEMIE-Geo.

Symbol

A— Area, m^2

B— Brine flow per evaporator, kg/s

Cp— Specific heat at constant pressure, kJ/kg EC

D— Vapor flow generated in each effect, kg/s

F— Feed flow for each effect, kg/s

h— Specific enthalpy, kJ/kg

LMTD— Logarithmic average temperature, °C

lts— Liters per second, l/s

M— Mass flow, kg/s

n— Number of evaporator tubes

T— Temperature, °C

ΔT—Temperature drop, °C

ΔT_l— Temperature drop in each evaporator, °C

U— Overall heat transfer coefficient, kW/m^2 EC

X— Salinity, ppm

η— Efficiency

λ— Latent heat of evaporation, kJ/kg

b— Brine

c— Condensate

cw— Seawater

d— Distilled

e— Evaporator

f— Feed

n— Last effect

ppm— Parts per million

v— Vapor

0—Reference state

REFERENCES

Abdelkareem, M.A., El Haj Assad, M., Sayed, E.T., & Soudan, B. (2018). Recent progress in the use of renewable energy sources to power water desalination plants. Desalination, 435, 97-113. DOI: 10.1016/j.desal.2017.11.018

Alkaisi, A., Mossad, R., & Sharifian-Barforoush, A. (2017). A review of the water desalination systems integrated with renewable energy. Energy Procedia, 110, 268-274. DOI: 10.1016/j.egypro.2017.03.138

Arango-Galván, C., Prol-Ledesma, R.M., & Torres-Vera, M.A. (2015). Geothermal prospects in the Baja California Peninsula. Geothermics, 55, 39–57. DOI: 10.1016/j.geothermics.2015.01.005

Arreguín, C.F.I., & Martín, D.A. (2000). Desalinización del agua. Ingeniería Hidráulica en México, 15(1, Enero-Abril), 27-49. Recuperado de http://www.revistatyca.org.mx/ojs/index.php/tyca/article/view/848/841

Arreguín, C.F.I., & López, P.M. (2015). Baja California y Quintana Roo: pioneros de la desalación en México. Consejo Consultivo del Agua, A.C. Recuperado de http://www.aguas.org.mx/sitio/index.php/blog/noticias/item/424-baja-california-y-quintana-roo-pioneros-de-la-desalacion-en-mexico

B2B Connect UAE. (2018). International Water Summit: Energy Efficient Desalination. Recuperado de https://www.internationalwatersummit.com/__media/Energy-Efficient-Desalination-2018.pdf

Báncora, A.C., & Prol, L.R.M. 2006. Mapa del flujo de calor en la Península y Golfo de California. Geos, 26(1), 22.

Barragán, R.M., Birkie, P., Portugal, E., Arellano, V.M., & Alvarez, J. (2001). Geochemical survey of medium temperature geothermal resources from the Baja California Peninsula and Sonora, México. Journal of Volcanology and Geothermal Research, 110, 101-119. DOI: 10.1016/S0377-0273(01)00205-0

Beron-Vera, F.J., & Ripa, P. (2002). Seasonal salinity balance in the Gulf of California. Journal of Geophysical Research: Oceans, 107, 1-15. DOI: 10.1029/2000JC000769

Bourouni, K. & Chaibi, M.T. (2005). Application of Geothermal Energy for Brackish Water Desalination in the South of Tunisia. Proceedings World Geothermal Congress. Congreso llevado a cabo en Antalya, Turquía.

Castro, R., Mascarenhas, A.S., Durazno, R., & Collins, C.A. (2000). Seasonal variation of the temperatura and salinity at the entrance to the Gulf of California, Mexico. Ciencias Marinas, 26(4), 561-583. Recuperado de http://www.redalyc.org/pdf/480/48002602.pdf

CONAGUA, Comisión Nacional del Agua. (2016). Estadísticas del agua en México, edición 2016.

CRE, Comisión Reguladora de Energía. (2011). Evaluación de los recursos geotérmicos de baja entalpía de la península de Baja California, México. Recuperado de http://www.cre.gob.mx/estudios/ce0111.pdf

Delgadillo-Hinojosa, F., Segovia-Zavala, J.A., Huerta-Díaz, M.A., & Atilano-Silvia, H. (2006). Influence of geochemical and physical processes on the vertical distribution of manganese in Gulf of California waters. Deep Sea Research Part I: Oceanographic Research Papers, 53(8), 1301-1319. DOI: 10.1016/j.dsr.2006.06.002

Dévora, I.G.E., González, E.R., & Ponce, F.N.E. (2012). Técnicas para desalinizar agua de mar y su desarrollo en México. Ra Ximhai, 8(2, mayo-agosto), 57-68. Recuperado de http://www.redalyc.org/articulo.oa?id=46123333006

Esparza, M. (2014). La sequía y la escasez de agua en México: Situación actual y perspectivas futuras. Secuencia, 89(mayo-agosto), 193-219. Recuperado de http://www.scielo.org.mx/pdf/secu/n89/n89a8.pdf

Flores-Luna, C., Romo-Jones, J.M., Vázquez-González, R., & López-Tipa, A., (1996). Exploración geoeléctrica con sondeos por transitorio electromagnético en la zona de Puertecitos, B.C. Residencia General de Cerro Prieto, Departamento de Exploración, pp. 38 (CFE. Internal Report-RGCP-CLS-007/95).

Ettouney, H. (2007). Developments in thermal desalination processes: design, energy, and costing aspects. Desalination, 214, 227–240.

Geankoplis C.J. (2003). Transport processes and separation process principles (4th ed.) Prentice Hall: Englewood Cliffs, NJ.

Ghaffour, N., Lattemann, S., Missimer, T., Choon Ng, K., Sinha, S., & Amy, G. (2014). Renewable energy-driven innovative energy-efficient desalination technologies. Applied Energy, 136, 1155-1165. DOI: 10.1016/j.apenergy.2014.03.033

Ghaffour, N., Bundschuh, J., Mahmoudi, H., & Goosen, M.F.A. (2015). Renewable energy driven desalination technologies: A comprehensive review on challenges and potential applications of integrated systems. Desalination, 365, 94-114. DOI: 10.1016/j.desal.2014.10.024

Hiriart Le Bert, G. (2009). Potencial energético del Alto Golfo de California. Boletín de la Sociedad Geológica Mexicana, 61(1), 143-146. DOI: 10.18268/BSGM2009v61n1a13

Ismail, T.M., Azab, A.K., Elkady, M.A., & Abo Elnas, M.M. (2016). Theoretical investigation of the performance of integrated seawater desalination plant utilizing renewable energy. Energy Conversion and Management, 126, 811-825. DOI: 10.1016/j.enconman.2016.08.002

Khalid, K.A., Antar, M.A., Khalifa, A., & Hamed, O.A. (2018). Allocation of thermal vapor compressor in multi effect desalination systems with different feed configurations. Desalination, 426, 164-173. DOI: 10.1016/j.desal.2017.10.048

Lavín, M.F., Beier, E. y Badán, A. (1997). Estructura hidrográfica y circulación del Golfo de California: Escalas estacional e interanual. Contribuciones de la Oceanografía Física en

México. Monogr. No. 3, Unión Geofísica Mexicana, pp. 139–169.

Lavín, M.F., & Sánchez, S. (1999). On how the Colorado River affected the hydrography of the upper Gulf of California. Continental Shelf Research, 19, 1545–1560. DOI: 10.1016/S0278-4343(99)00030-8

Lavín, M.F., & Marinone, S.G. (2003). An overview of the physical oceanography of the Gulf of California. Nonlinear Processes in Geophysical Fluid Dynamics, 173-204. DOI: 10.1007/978-94-010-0074-1_11

Lynn, S.M. (1978). Coastal warm spring systems along Northeastern Baja California (tesis de maestría). San Diego State University, Estados Unidos.

Manenti, F., Masi, M., Santucci, G., & Manenti, G. (2013). Parametric simulation and economic assessment of a heat integrated geothermal desalination plant. Desalination, 317, 193-205. DOI: 10.1016/j.desal.2013.02.027

Montes, J.M., Lavín, M.F., & Parés-Sierra, A.F. (2016). Seasonal Heat and Salt Balance in the Upper Gulf of California. Journal of Coastal Research, 32 (4), 853-862. DOI: 10.2112/JCOASTRES-D-14-00192.1

Nava, C.E., & Hiriart Le Bert, G. (2008). Desalación de agua con energías renovables, CDMX, México: Instituto de Ingeniería, UNAM.

Suárez, A.M.C. (2004). Evaluación del potential, biogenesis y características esenciales de los sistemas geotérmicos submarinos en México. Geotermia, 17(1), 31-43. Recuperado de http://132.248.9.34/hevila/Geotermia/2004/vol17/no1/4.pdf

Vázquez-Figueroa, V., Canet, C., Prol-Ledesma, R.M., Sánchez, A., Dando, P., Camprubi, A., Robinson, C.J., & Hiriart Le Bert, G. (2009). Batimetría y características hidrográficas (Mayo, 2007) en las Cuencas de Consag y Wagner, Norte del Golfo de California, México. Boletín de la Sociedad Geológica Mexicana, 61, 119-127. DOI: 10.1016/j.sedgeo.2010.05.004

WWAP (Programa Mundial de las Naciones Unidas de Evaluación de los Recursos Hídricos) /ONU-Agua. (2018). Informe Mundial de las Naciones Unidas sobre el Desarrollo de los Recursos Hídricos 2018: Soluciones basadas en la naturaleza para la gestión del agua. París, UNESCO.